Philosophical Magazine
Publication details, including instructions for authors and subscription information:
http://www.tandfonline.com/loi/tphm20

New ring-like models and ab initio DFT study of the medium-range structures, energy and electronic properties of $GeSe_2$ glass

R. Holomb [a], V. Mitsa [a], S. Akyuz [b] & E. Akalin [c]

[a] Institute of Solid State Physics and Chemistry, Uzhhorod National University, Uzhhorod, 88000, Ukraine

[b] Physics Department, Istanbul Kultur University, Bakirkoy, Istanbul, 34156, Turkey

[c] Physics Department, Istanbul University, Vezneciler, Istanbul, 34134, Turkey

Published online: 11 Mar 2013.

To cite this article: R. Holomb, V. Mitsa, S. Akyuz & E. Akalin (2013) New ring-like models and ab initio DFT study of the medium-range structures, energy and electronic properties of $GeSe_2$ glass, Philosophical Magazine, 93:19, 2549-2562, DOI: 10.1080/14786435.2013.778426

To link to this article: http://dx.doi.org/10.1080/14786435.2013.778426

Philosophical Magazine, 2013
Vol. 93, No. 19, 2549–2562, http://dx.doi.org/10.1080/14786435.2013.778426

New ring-like models and *ab initio* DFT study of the medium-range structures, energy and electronic properties of $GeSe_2$ glass

R. Holomb[a]*, V. Mitsa[a], S. Akyuz[b] and E. Akalin[c]

[a]*Institute of Solid State Physics and Chemistry, Uzhhorod National University, Uzhhorod 88000, Ukraine;* [b]*Physics Department, Istanbul Kultur University, Bakirkoy Istanbul, 34156, Turkey;* [c]*Physics Department, Istanbul University, Vezneciler Istanbul, 34134, Turkey*

(*Received 23 December 2011; final version received 16 February 2013*)

Ab initio DFT calculations were performed on Ge_nSe_m nanoclusters ($n = 2$, 3, 5, 6, 12; $m = 6$–9, 14, 16, 30) that represent the local structure of $GeSe_2$ glass and on some 'defect' Ge_nSe_m clusters that are thought to be related to the inhomogeneity of the structure at the nanoscale. The optimal geometries, total energies and their derivatives as well as the electronic properties of Ge_nSe_m nanoclusters were calculated using traditional DFT method. In addition, the TD-DFT method has been applied to calculate the electronic band gaps of the clusters. The calculated physico-chemical properties of Ge_nSe_m nanoclusters and their couplings with the local-and medium-range order structure formations in $GeSe_2$ glass are analysed and discussed.

Keywords: *ab initio*; DFT; $GeSe_2$ glass; finite clusters

1. Introduction

Amorphous (a) and glassy (g) semiconducting chalcogenides attract a great interest due to their remarkable structural, electronic and optical properties demonstrating a wide range of potential applications in optoelectronics [1,2]. For example, the reversible and irreversible electronic and optical switching in chalcogenide glasses (ChG) discovered by Ovshinsky [3] was one of the greatest advancements of technology stimulating the intensive investigations of non-crystalline semiconductors. Due to their large infrared (IR) transparency, ChG-based fibres can be used for transmitting high power of IR light and IR biosensing [4,5]. The light sensitivity and photo-structural transformations of ChGs [6] are key features of phase-change memory [7]. In addition, ChGs exhibit large third-order optical non-linearities and they can be the excellent candidates as the base of modern photonic devices such as all optical non-linear switching, data signal processing, optical regeneration, Raman and parametric amplification, etc. [8–12].

Modern technology requires quantitative understanding of structure, properties and induced processes occurring at the nanoscale regions. The lack of translational symmetry in glassy chalcogenides limits the structural information obtained from diffraction experiments. However, the correlations existing between nearest neighbours allow us to characterise the non-crystalline materials at the so-called short-range order (SRO) by

*Corresponding author. Email: holomb@ukr.net

analysing the total and partial structure factors $S(Q)$ and its Fourier counterparts, the atomic partial distribution functions $g(r)$ obtained from the X-ray or neutron scattering experiments [13–16]. Application of the isotopic substitution method as a further advancement in neutron diffraction allows the experimental separation of full set of partial structure factors [15–18]. In addition, the diffraction method can also give structural information on the ordering at much larger distances associated with medium (also termed intermediate)-range order (MRO) as manifested by the appearance in the measured diffraction patterns of a so-called first sharp diffraction peak [19,20]. Moreover, the recent diffraction experiments reveal the additional characteristic length scale beyond 20 Å associated with the new level of ordering (extended range order) in the glass structure [17].

The structure of ChGs at length scale associated with SRO can also successfully be studied by means of photoelectron spectroscopy and inelastic scatterings [21–24]. Moreover, Raman spectroscopy may provide some additional information extending our understanding of non-crystalline structure to the second and larger coordination shells [6,23–25]. However, at present, there is no unique experimental technique to investigate amorphous structure that provides direct structural information in so-called MRO length scale. Therefore, nowadays much attention is paid on structural modelling, molecular dynamics (MD) simulations and *ab initio* studies of the amorphous structures and their properties. A quantitative understanding of optical excitations, absorption and structural transformations of molecules, clusters and nanocrystals is very important for modern photochemistry, spectroscopy and for the designing of optical materials.

The stoichiometric $GeSe_2$ glass composition has been the subject of great scientific and technological interest as promising material for IR optical and non-linear photonics applications [9,26–32]. In addition, g-$GeSe_2$ shows various kinds of light-induced structural changes such as photo-bleaching, photo-crystallization, photo-induced diffusion [33,34]. The photomodification properties of dichalcogenides can be applied to the branch couplers, interferometers, waveguides, nanolenz and photo-resist materials for the micro- and nanofabrication. Also, $GeSe_2$ is 'canonical' model object of the binary Ge–Se glass system with the complex structure, particularly in view of achieving a description of the relationship between the short- and medium-range ordering, local dimensionality and structural transition at the atomic scale and the resulting electronic and optical properties [35,36]. Therefore, the aim of this work is to study the formation and organisation of g-$GeSe_2$ structures as well as to study the evolution of their electronic properties by using cluster modelling and *ab initio* DFT calculations. This study is focused on gas-phase Ge–Se clusters that have size- and orientation-dependent geometries obtained from the structure of $GeSe_2$ monolayer. In addition, few models with homopolar bond and non-typical geometries in comparison with $GeSe_2$ crystal have been proposed and studied by using *ab initio* calculations.

2. Cluster modelling and calculation details

Structural investigations show that the main SRO structures of amorphous state with covalently bonded network are typical to those found in their crystalline analogue. Therefore, the examination of the structure of corresponding crystals is very important for the first-stage modelling of the local amorphous structures. There are two well-known crystalline forms of germanium diselenide. The $GeSe_4$ tetrahedron in the

structure of low- temperature α-form of $GeSe_2$ is mutually connected by their corners and forms the three-dimensional crystal network [37,38]. However, high-temperature β-form generates two-dimensional (2D) network built-up by combination of $GeSe_4$ tetrahedra with corner- and edge-sharing geometries [39–41]. In this network, the parallel endless chains of corner-sharing tetrahedra are linked together by edge-sharing tetrahedra (Figure 1). Thus, the local SRO structures representing the beta form of $GeSe_2$ crystal are corner- and edge-sharing tetrahedra (models I and II). Further extending the length scale to the lager coordination spheres leads to an increase in the degree of freedom in the formation of amorphous structures. In this case, the structural formation may be studied in detail by *ab initio* method using a gas-phase cluster approach. The larger cluster which can be found in the crystal structure of $GeSe_2$ is a six-member ring consisting three $GeSe_4$ tetrahedra connected by their corners (III). It should be noted here that two edge-sharing tetrahedra can also be classified as four-member ring. Models IV and V represent two six-member rings selected from two directions of 2D network of β-$GeSe_2$ crystal. In the first case the rings are connected by common Ge while in the other model rings are connected via the edge-sharing block. The largest cluster obtained from the crystal structure of $GeSe_2$ monolayer (VI) consists of a big 16-member ring.

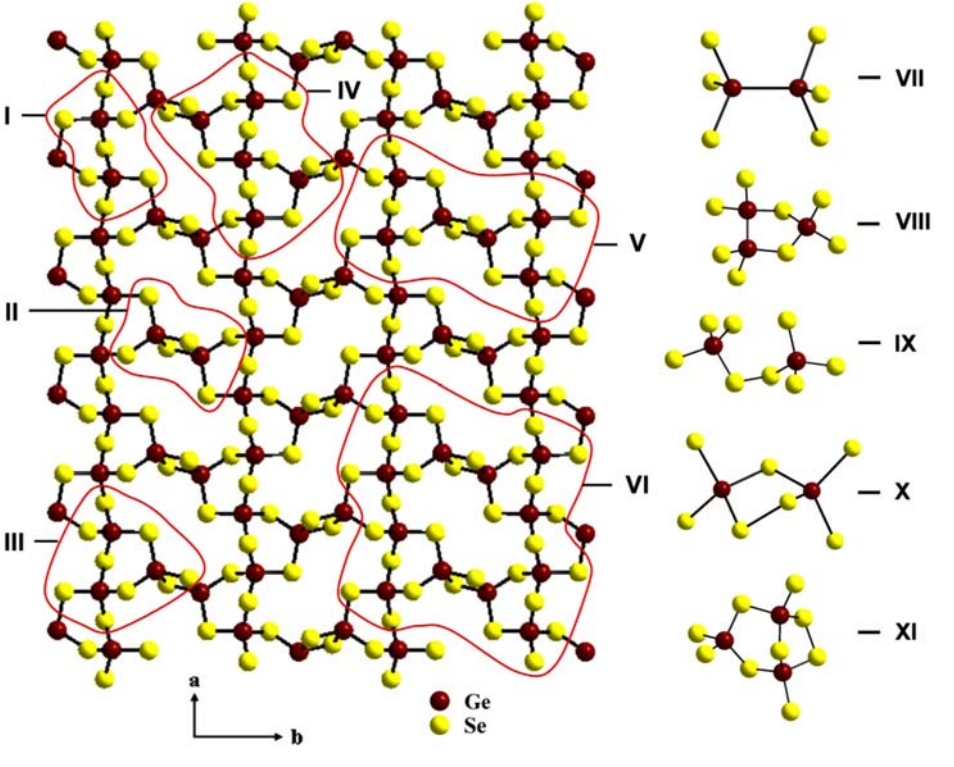

Figure 1. (colour online) The crystal structure of high- temperature (β) $GeSe_2$ monolayer [41] with the selected $Ge_nSe_mH_p$ cluster models (I–VI) (left) and the 'defect' $Ge_nSe_mH_p$ cluster geometries with homopolar Ge–Ge (VII–VIII) and Se–Se (IX–XI) bonds (right). Saturating hydrogen atoms and corresponding bonds are not shown for clarity.

It is well known that the structure of amorphous state is very sensitive to the synthesis condition and production technology [23,35]. The significant difference between amorphous and crystalline states in the structure and in the properties could be due to formation of 'defects' which include either homopolar (or so called 'wrong') bonds in binary systems or a non-typical chemical coordination and non-typical geometry in comparison to the crystals of corresponding compositions. Such Ge–Ge and Se–Se correlations have been experimentally observed in the diffraction studies of $GeSe_2$ glass at typical homopolar single-bond distances of 2.42 and 2.32 Å, respectively, while the measured bond length of Ge–Se is 2.36 Å [15,16]. Also, from the calculated coordination numbers for the Ge–Se, Ge–Ge and Se–Se bonds it was found that the Ge and Se atoms in the g-$GeSe_2$ network are four- and two-fold coordinated, respectively [15,16]. The *ab initio* methods are very useful to analyse different possible 'defect' configurations. Here, we represent few possible models with homopolar Ge–Ge (VII–VIII) and Se–Se (IX–XI) bonds. The simplest model of Ge–Ge bond can be seen in the hypothetical cluster, so-called ethane-like geometry (VII) [42]. Similar way homopolar Se–Se bond can be realized as a linkage between two $GeSe_4$ tetrahedra (IX). There is also possibility of Se–Se bond formation on the edge of the so-called outrigger raft structure (model XI represents the part of this structure) [43]. Recent investigation of the structure of Ge_4Se_9 crystal shows that there is another possibility to form Se–Se bond through $Ge_2Se_{3+4/2}$ cluster (X) which substitute edge-sharing blocks in 2D crystalline network of β-$GeSe_2$ [44,45]. This cluster together with the model VIII represents five-member rings with incorporated Se–Se and Ge–Ge bonds, respectively. *Ab initio* MD simulations show that in addition to six- and four-member rings the other types of *i*-member rings ($i = 3$–12) in the structure of liquid and glassy $GeSe_2$ can be seen [46–49].

The dangling bonds of the surface atoms of the selected finite Ge_nSe_m models (Figure 1) were saturated by hydrogen atoms for a better representation of the cluster boundaries and H-terminated $Ge_nSe_mH_p$ nanoclusters used for further *ab initio* calculations. The computational part consists of *ab initio* DFT calculations performed using the Gaussian-03 quantum-chemical programme package [50]. The self-consistent DFT field method [51] was applied for geometry optimizations of the clusters using the Berny optimization procedure. The LANL2DZdp ECP basis set of Hay and Wadt [52] with polarization function [53] was used for the Ge, Se and H atoms together with the corrected exchange functional proposed by Becke [54] and the gradient-corrected correlation functional of Lee, Yang, and Parr [55] (BLYP). Subsequently, second derivative calculations verified the obtained structures as true energy minimum geometries.

The electronic properties in terms of molecular orbitals (MO) of fully optimized $Ge_nSe_mH_p$ clusters were studied by standard DFT method which is known to be efficient for the calculation of ground-state properties. Furthermore, using the highest occupied and lowest unoccupied MOs (HOMO and LUMO) energies, it is possible to estimate the electronic HOMO–LUMO band gap (ΔE_g^{H-L}) of the clusters. However, this method may give significant inaccuracy in calculated energy values of unoccupied states. Therefore, the excited-state properties were also studied using time-dependent DFT method (TD-DFT) in which the time-dependent electron density is used [56–58]. In this case, the band gaps of the clusters were estimated by the energy difference between low-lying ground and first excited-state energies (ΔE_g^{gr-ex}).

3. Results and discussion

3.1. *Optimal geometry, total and formation energies*

The averaged Ge–Se bond length (2.43 Å) is almost the same for all optimized $Ge_nSe_mH_p$ clusters and systematically larger by about 0.07 Å in comparison with the average Ge–Se bond length found in $GeSe_2$ crystal [41]. Calculations show that the Ge–Ge bond (2.53 Å) is about 0.1 Å longer compared to the Ge–Se bond length while Se–Se bond (~2.42 Å) is only very slightly shorter. The calculated Ge–Se, Ge–Ge and Se–Se bond distances are systematically overestimated by ~3–4% in comparisons with the experimental values and follow the trend obtained from recent neutron diffraction studies of $GeSe_2$ glass [15,16]. Our analysis show that such small overestimation in bond distances is mainly due to exchange-correlation part of the energy functional used for calculations as it was also pointed out in [59] rather than due to neglecting of many body interaction in cluster approximation.

The calculated mean values of Se–Ge–Se bond angles of clusters are very close to 109.5° which is near perfect tetrahedral angle of 109.47°. The maximal deviation (~11.4°) is observed for clusters with edge-sharing geometry where Se–Ge–Se angle decreases up to 98.1°. Also, the calculated Ge–Ge–Se bond angle within ethane-like cluster is very close to ideal tetrahedron. However, the mean Ge–Se–Ge bond angles in edge-sharing geometry II (81.9°) and clusters containing edge-sharing block(s) V and VI (96.9° and 97.5°, respectively) are systematically smaller compared to those of corner-sharing $GeSe_4$ tetrahedra I (104.0°), III (103.7°) and IV (103.8°). Smaller Ge–Se–Ge (98.5°, 98.1° and 99.8°) are characteristics of five-member rings with homopolar Ge–Ge and Se–Se bonds (models VIII, X and XI, respectively). The mean Ge–Se–Se angles of clusters with Se–Se bond (IX, X and XI) were calculated at 103.3°, 97.0°, 98.9°, respectively. Figure 2 shows the distributions of optimized Ge–Se–Ge, Se–Ge–Se, Se–Se–Ge and Ge–Ge–Se bond angles of $Ge_nSe_mH_p$ cluster models. As can be seen the Ge–Se–Ge bond angle distributions of the bigger clusters (models V and VI) based on the structure of β-$GeSe_2$ monolayer show two peaks at 81.2° and 102.1°. These values are in very good accordance with the Ge–Se–Ge angles of 80° and 98° obtained by Salmon from neutron diffraction studies of $GeSe_2$ glass [18]. The first peak arises from edge-sharing blocks (four-member rings) while the second peak results from six-member ring structures and/or corner-sharing tetrahedra. Similar but more broadened Ge–Se–Ge bond angle distribution was obtained by Massobrio et al. from the results of MD simulation [49]. Our results show that such broadening in the bond angle distribution can be due to formation of 'defect' clusters (models VIII, X and XI). As can be seen from Figure 2, the contribution of such clusters will lead to broadening of the main peak at 102.1° and to decrease in a valley between two peaks (81.2° and 102.1°). The evolution of Se–Ge–Se bond angle distributions of β-$GeSe_2$-based clusters (models I–VI) is more complex and contain three peaks at ~99.9°, 104.9° and 112.3° (Figure 2). For the bigger models (V and VI), the Se–Ge–Se bond angle distributions are broadened, asymmetric and very similar to that obtained from MD study of g-$GeSe_2$ [49].

For further classification of the structures of Ge–Se clusters, we have calculated their energy characteristics. Table 1 summarizes the total energy (E_{tot}) of the $Ge_nSe_mH_p$ clusters. In general, the total energy of the cluster can be expressed as follows:

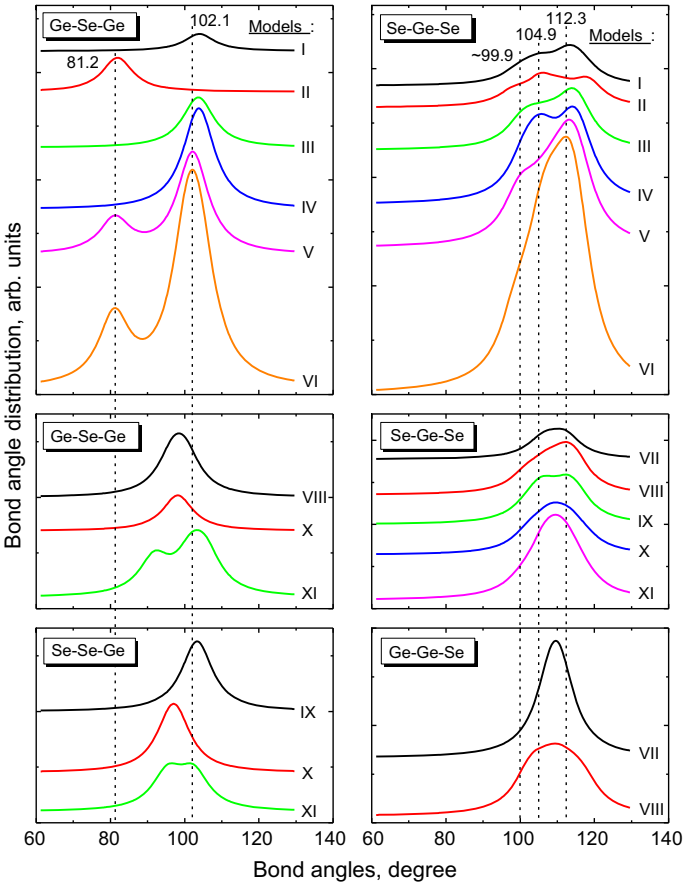

Figure 2. (colour online) The distributions of optimized Ge–Se–Ge, Se–Ge–Se, Se–Se–Ge and Ge–Ge–Se bond angles of $Ge_nSe_mH_p$ cluster models.

Table 1. Total (E_{tot}) energies of $Ge_nSe_mH_p$ clusters and formation (E_{form}), weighted E_a and E_b energies of Ge_nSe_m clusters calculated using DFT/BLYP/LANL2DZ (d,p) ECP method. All energy values are given in Hartree.

Cluster model	E_{tot}	E_{form}	E_a	E_b
I	−75.7434	−0.8070	−0.0897	−0.1009
II	−65.3489	−0.8555	−0.1069	−0.1069
III	−98.0269	−1.2868	−0.1072	−0.1072
IV	−152.9855	−2.1950	−0.1155	−0.1097
V	−175.2630	−2.6688	−0.1213	−0.1112
VI	−329.7426	−5.4403	−0.1295	−0.1133
VII	−66.5008	−0.6519	−0.0815	−0.0931
VIII	−88.7849	−1.1323	−0.1029	−0.1029
IX	−84.9668	−0.9428	−0.0943	−0.1048
X	−74.5734	−0.9925	−0.1103	−0.1103
XI	−96.8491	−1.4645	−0.1220	−0.1127

$$E_{\text{tot}} = \sum E_{\text{at}} + \sum E_{\text{bond}}, \tag{1}$$

where E_{tot}, E_{at} and E_{bond} are total energy of cluster, energy of the elements that are constituents of the cluster, and bond energy, respectively.

However, the calculated total energy includes saturating hydrogen energies and corresponding Se–H bond energies and, therefore, cannot directly be used for comparisons. By calculating hydrogen and Se–H bond energies and using Equation (1), it is possible to calculate the formation energy (E_{form}) of Ge_nSe_m cluster:

$$E_{\text{form}} = E_{\text{tot}} - \sum E_{\text{Ge}} - \sum E_{\text{Se}} - \sum E_{\text{H}} - \sum E_{\text{Se–H}} \tag{2}$$

The absolute value of formation energy increases with the increasing cluster size (number of bonds) as shown in Figure 3(a) (models I–VI). On the other hand,

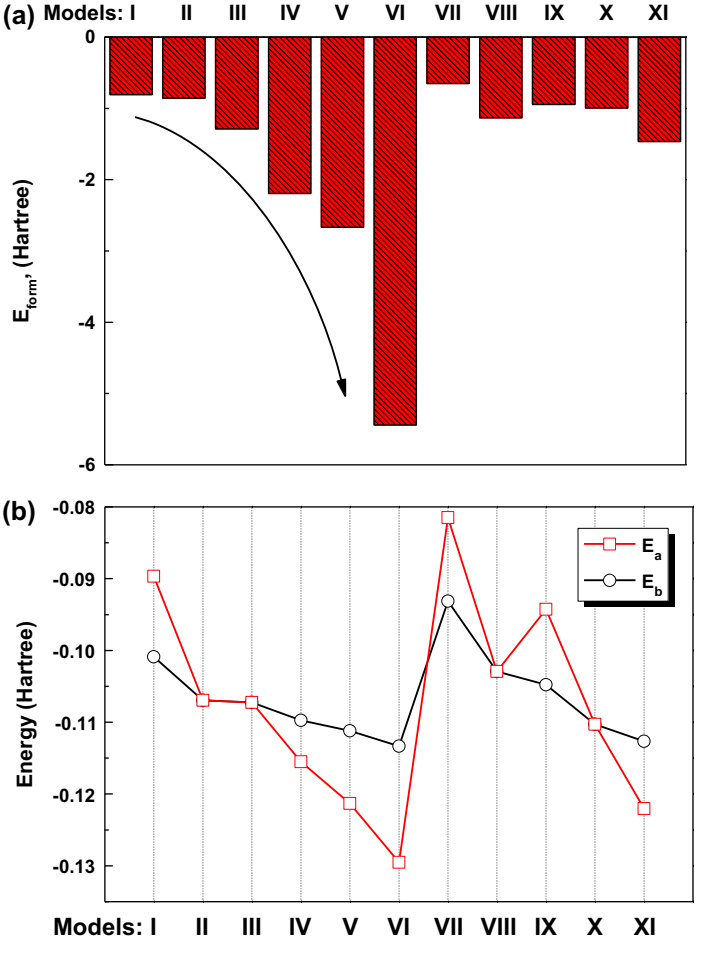

Figure 3. (colour online) Formation energies of the Ge_nSe_m nanoclusters as a function of cluster size and/or geometry (a) and weighted formation energies, E_a (E_{form} per atom) and E_b (E_{form} per bond) (b).

the comparison of the formation energy of corner- and edge-sharing bi-tetrahedra containing eight Ge–Se bonds (I and II) immediately lead to the conclusion that the edge-sharing geometry structure is energetically more favourable (Table 1).

For further analysis of the energy and stability of Ge_nSe_m nanoclusters, we have calculated weighted formation energy values, $E_a = E_{form}/N_a$ and $E_b = E_{form}/N_b$, where N_a and N_b are the numbers of atoms and bonds, respectively (Table 1). Obtained data for models IV and V are further evidence that the cluster contained edge-sharing block is energetically more stable. Within studied clusters, E_a and E_b demonstrate similar energy trends (Figure 3(b)). For the models I–VI, both values continuously decrease with the increasing size indicating the sizedependence in cluster stability: the bigger the cluster the lager the stability.

The analysis of E_a shows that the formations of corner-sharing tetrahedra itself (I), Ge–Ge bond within ethane-like cluster (VII) and bridge Se–Se bond between two $GeSe_4$ tetrahedra (IX) are energetically not preferred. On the other hand, the formation of six-member ring (III) from three corner-sharing tetrahedra or incorporation of such Ge–Ge bond in five-member ring structure (VIII) significantly decreases the characteristic energy. Also, the formation of five-member ring with Se–Se bond (X) is more favourable in comparison with model IX. The characteristic energy decreases further for the model XI with the Se–Se bond at the cluster end. This structure can also be viewed as shared six- and five-member rings. Therefore, the analysis of Ge_nSe_m energies indicates that the ring is a more stable model for the local structure of $GeSe_2$ in comparison to models based on corner-sharing connection of $GeSe_4$ tetrahedra. Thus, edge-sharing tetrahedra (four-member ring) and six-member ring are the most stable local structures found in $GeSe_2$ glass. This result is in good agreement with the ring statistics obtained from MD simulations of glassy $GeSe_2$ [47,49]. In addition, the five-member rings with Ge–Ge and Se–Se bonds are energetically the most preferred models presenting homopolar bonds. The later cluster (X) is also found in Ge_4Se_9 crystal [45]. Moreover, the mean value of characteristic energies (E_a) of the models VIII and X which is calculated to be at -0.1066 Hartree correspond to the calculated energies of stable four- and six-member rings (Table 1). Therefore, the formation of five-member ring with homopolar Ge–Ge bond and five-member ring containing Se–Se bond in g-$GeSe_2$ can be realized by the balance between their energies.

MD simulations of $GeSe_2$ glass [47,49] revealed that five-member rings with Se–Se bond were more abundant in number than five-member rings with Ge–Ge bond. This result is supported by our calculation in which the formation of ring with Se–Se bond is energetically more favourable in comparison to the rings having Ge–Ge bond and this indicates the interconnection between the probability of structural organization and the energy characteristics.

3.2. *MO and electronic properties*

Calculated HOMO and LUMO energies are tabulated in Table 2. The HOMO and LUMO energies of $Ge_nSe_mH_p$ clusters calculated using DFT method cover ranges from -5.41 to -5.87 eV and from -3.10 to -3.62 eV, respectively. The systematically larger HOMO value within models is found in five-member rings with Se–Se bond (X and XI). Even brief analysis of differences between HOMO and LUMO energies (ΔE_g^{H-L}) for models I–VI show the size dependence in energy gap formation: an increase in

Table 2. Occupied and unoccupied MO energies (eV) and HOMO–LUMO band gaps (ΔE_g^{H-L}) of Ge_nSeH_p clusters calculated using traditional DFT together with the band gaps (ΔE_g^{gr-ex}) calculated using TD-DFT method.

	DFT			TDDFT
Cluster model	HOMO	LUMO	ΔE_g^{H-L}	ΔE_g^{gr-ex}
I	−5.80	−3.10	2.70	2.49
II	−5.87	−3.33	2.55	2.40
III	−5.81	−3.17	2.64	2.44
IV	−5.81	−3.37	2.45	2.20
V	−5.72	−3.43	2.29	2.10
VI	−5.76	−3.62	2.14	1.91
VII	−5.72	−3.10	2.62	2.61
VIII	−5.82	−3.18	2.64	2.43
IX	−5.74	−3.22	2.52	2.39
X	−5.58	−3.19	2.38	2.24
XI	−5.41	−3.35	2.06	1.95

cluster size lead to a decrease in band gap. Therefore, to compare the band gaps of the clusters that have different geometries with each other, it is better to use models having the similar number of atoms/bonds. When a comparison is made between ΔE_g^{H-L} of models I and II and models IV and V, it is clearly seen that the systematically smaller band gap belonged to the models with edge-sharing geometry. The same trend in band gaps is observed when TD-DFT method (ΔE_g^{gr-ex}) was used for calculations. Figure 4 shows that the HOMO state is formed by Se(p) non-bonding (LP) molecular orbital and the LUMO state is Ge(s)–Se(p) σ^* antibonding molecular orbital.

The formation of Ge–Ge bond (VII and VIII) in the structure of amorphous $GeSe_2$ does not affect the formation of additional states that decrease the pseudogap of

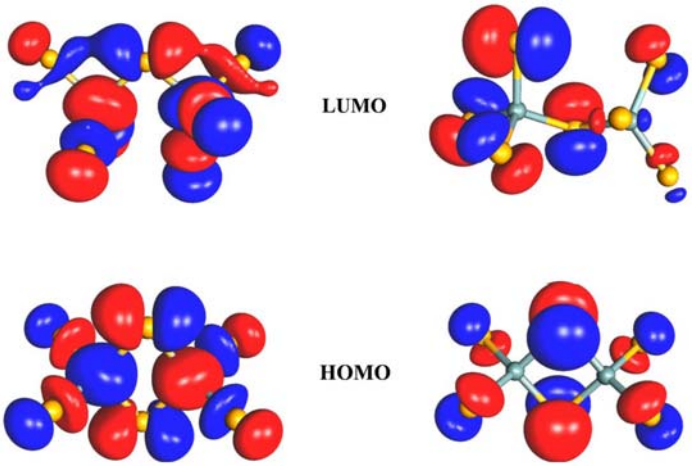

Figure 4. (colour online) Highest occupied and lowest unoccupied MOs of corner- (left) and edge-sharing (right) $GeSe_4$ bi-tetrahedra: HOMO – Se(p) non-bonding (LP) MOs; LUMO – Ge(s) and Se(p) σ^* antibonding MOs.

amorphous material (Table 2). Examining the role of Ge–Ge bonds on density of states (DOS) of 4:2 coordinated Ge_xSe_{1-x} compounds performed in [60], we see that the increasing number of Ge–Ge bonds mainly leads to broadening of the Ge 4s band. In contrast to Ge–Ge bond, the formation of Se–Se bond leads to a decrease in band gap values. The smallest band gap, 2.06 eV, was calculated for model XI with Se–Se bond at the end. MO analysis indicates that this is mainly due to the increase in highest occupied state energy value of Se (p) non-bonding MO localized on Se–Se bond. The formation of such structures in glass matrix leads to the formation of additional states in pseudogap of amorphous materials as it can be seen from Figure 5.

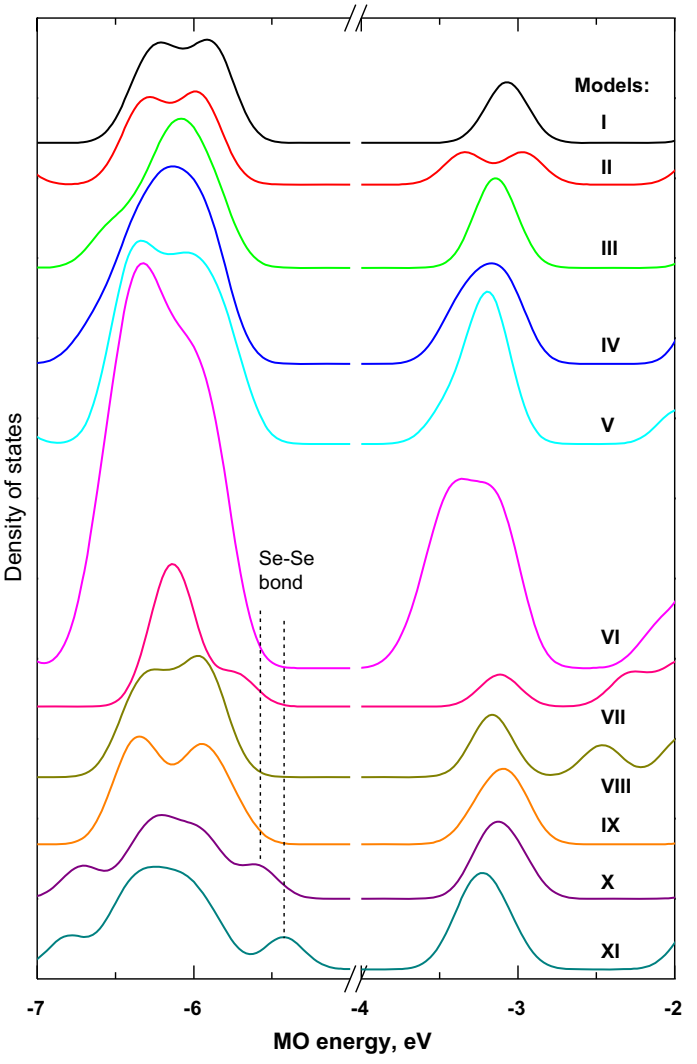

Figure 5. (colour online) Evolution of theoretical electronic DOS of $Ge_nSe_mH_p$ nanoclusters. (DOS spectra were simulated by integration of broadened (FWHM = 0.3 eV) Gaussian bands centred at each calculated eigenvalue).

3.3. *Energy and band gap as a function of geometrical parameters*

The energy characteristics and electronic properties calculated for optimized structures of different Ge_nSe_m nanoclusters correlate with their geometrical parameters. In order to study such dependences in detail, we have performed additional calculations that consists angle-dependent potential energy scans and optimizations. As shown in Figure 6(a), the significant decreases in band gaps calculated for edge-sharing tetrahedra and ring structure (II–III) can directly be correlated with decreasing of Ge–Se–Ge angle (φ_1) from 103.7° to 81.9° (see Section 3.1). The HOMO and LUMO states and corresponding band gap are practically the same for models III and VIII. Therefore, the formation of Ge–Ge bond cannot influence significantly the pseudogap of amorphous $GeSe_2$. According to our previous studies of GeS_2 glasses, the significant decreases in band gap can be due to the phase separation of Ge-rich structures with three coordinated Ge and S characteristics of GeS crystal [23].

However, the decreasing of the band gap by the formation of Se–Se bond in five-member rings (X and XI) can be connected with the formation of additional states in experimental DOS spectra of non-crystalline $GeSe_2$. Furthermore, the HOMO–LUMO band gaps of these two clusters with Se–Se bond were found to be very sensitive to the geometrical configuration: the gaps were calculated to be 2.38 and 2.06 eV for models X and XI, respectively. Our analysis shows that the minor changes of Ge–Se–Se angles (φ_2: 97.0° and 98.9°) within clusters cannot be responsible for the drastic changes in band gap values (Figure 6(b)). However, the analysis shows that Ge–Se–Se–Ge dihedral angles of models X ($\psi = 52.1°$) and XI ($\psi = 34.3°$) are responsible for the significant decrease in the band gap value (from 2.23 eV to 2.05 eV) (see Figure 6(c)). Therefore, the drastic decreases in band gap of Ge_nSe_m clusters can directly be connected to the decrease in Ge–Se–Se–Ge dihedral angle. The formation of Se–Se bonds in the structure of $GeSe_2$ and Se-rich Ge–Se glasses may increase the degree of freedom of structural matrix, thus resulting in different possible conformations of Ge–Se–Se–Ge dihedral angle. The conformational changes (excluding bond breaking) around chalcogen-chalcogen bonds induced by laser radiation can be responsible for effects of reversible photo-induced changes in electronic structure of amorphous chalcogenides such as photo darkening.

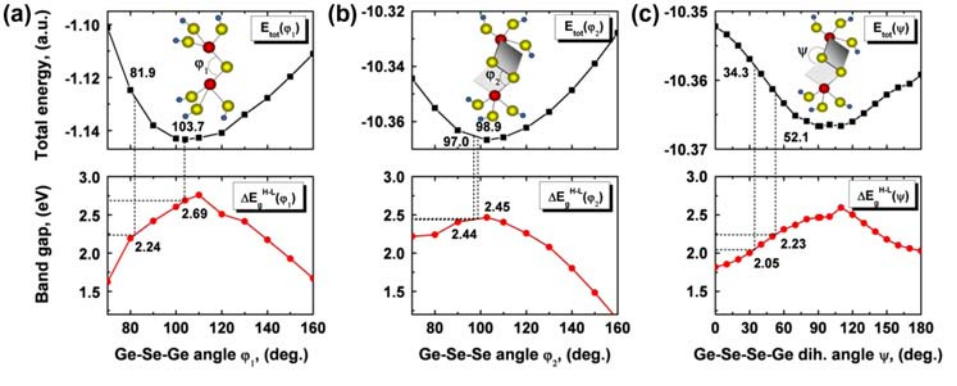

Figure 6. (colour online) Total energy and electronic properties of corner-sharing bi-tetrahedra and $GeSe_4$ bi-tetrahedra connected by Se–Se bridge as a function of Ge–Se–Ge angle (φ_1), Ge–Se–Se angle (φ_2) and Ge–Se–Se–Ge dihedral angle (ψ).

4. Conclusion

The geometry and electronic properties of Ge_nSe_m nanoclusters representing the local and MRO structures of $GeSe_2$ crystal have been calculated by using *ab initio* DFT and TD-DFT methods. The 'defect' cluster models with homopolar Ge–Ge and Se–Se bonds that are thought to be related to the structural inhomogeneity found in $GeSe_2$ glass have also been proposed and studied in detail.

The analysis of total cluster energies and their derivatives show the preference in formation of four-, six-member rings and bigger clusters that are topologically similar to β-$GeSe_2$. Formations of Ge–Ge and Se–Se bonds are energetically favourable. They prefer to be incorporated in five-member rings rather than in form of ethane-like cluster and cluster with Se–Se bridge itself.

MO study of optimized four- and six-member ring Ge_nSe_m clusters and angle-dependent calculations show a correlation between band gap value and Ge–Se–Ge bond angle: the smaller the angle the narrower the band gap. The formation of Ge–Ge bond has only negligible effect on band gap. However, the formations of Se–Se bond significantly decrease the band gap value giving additional states in DOS. The magnitudes of band gap changes are found to correlate with Ge–Se–Se–Ge dihedral angle rather that Ge–Se–Se bond angle.

Acknowledgment

This work was performed within Ukrainian-Turkish collaboration in Science and Technology (Project Numbers M85-2010 and TUBITAK-109T643).

References

[1] I. Fekeshgazi, K. May, V. Mitsa and A. Vakaruk, *Physics and applications of non-crystalline semiconductors*, in *Optoelectronics*, A. Andriesh and M. Bertolotti, eds., Kluwer Academic Publishers, Dordrecht, 1997, Vol. 36, p.243.
[2] M.F. Thorpe and L. Tichý (eds.), *Properties and Applications of Amorphous Materials*, in *Proceedings of the NATO Advanced Study Institute, NATO Science Series II: Mathematics, Physics and Chemistry*, Kluwer, Dordrecht, 2001.
[3] S.R. Ovshinsky, Phys. Rev. Lett. 21 (1968) p.1450.
[4] J.S. Sanghera, I.D. Aggarwal, L.B. Shaw, L.E. Busse, P. Thielen, V. Nguyen, P. Pureza, S. Bayya and F. Kung, J. Opt. Adv. Mater. 3 (2001) p.627.
[5] M.-L. Anne, J. Keirsse, V. Nazabal, K. Hyodo, S. Inoue, C. Boussard-Pledel, H. Lhermite, J. Charrier, K. Yanakata, O. Loreal, J. Le Person, F. Colas, C. Compère and B. Bureau, Sensors 9 (2009) p.7398.
[6] R. Holomb, V. Mitsa, O. Petrachenkov, M. Veres, A. Stronski and M. Vlček, Phys. Status Solidi C 8 (2011) p.2705.
[7] T. Ohta, J. Opt. Adv. Mater. 3 (2001) p.609.
[8] A. Zakery and S.R. Elliott, *Optical nonlinearities in chalcogenide glasses and their applications*, Springer Series in Optical Sciences, Vol. 135, 2007.
[9] V. Ta'eed, N.J. Baker, L. Fu, K. Finsterbusch, M.R.E. Lamont, D.J. Moss, H.C. Nguyen, B.J. Eggleton, D.-Y. Choi, S. Madden and B. Luther-Davies, Opt. Express 15 (2007) p.9205.
[10] R.P. Wang, S.J. Madden, C.J. Zha, A.V. Rode and B. Luther-Davies, J. Appl. Phys. 100 (2006) p.063524.

[11] V. Mitsa, R. Holomb, M. Veres, A. Marton, I. Rosola, I. Fekeshgazi and M. Koós, Phys. Status Solidi C 8 (2011) p.2696.
[12] B.J. Eggleton, B. Luther-Davies and K. Richardson, Nat. Photonics 5 (2011) p.141.
[13] V. Petkov, J. Am. Ceram. Soc. 88 (2005) p.2528.
[14] A. Zeidler, J.W.E. Drewitt, P.S. Salmon, A.C. Barnes, W.A. Crichton, S. Klotz, H.E. Fischer, C.J. Benmore, S. Ramos and A.C. Hannon, J. Phys.: Condens. Matter 21 (2009) p.474217.
[15] I. Petri, P.S. Salmon and H.E. Fisher, Phys. Rev. Lett. 84 (2000) p.2413.
[16] P.S. Salmon and I. Petri, J. Phys.: Condens. Matter 15 (2003) p.S1509.
[17] P.S. Salmon, R.A. Martin, P.E. Mason and G.J. Cuello, Nature 435 (2005) p.75.
[18] P.S. Salmon, J. Phys.: Condens. Matter 19 (2007) p.455208.
[19] S.C. Moss and D.L. Price, in *Physics of Disordered Materials*, D. Adler, H. Fritzsche and S. R. Ovshinsky, eds., Plenum, New York, 1985, p.77.
[20] S. Susman, D.L. Price, K.J. Volin and R.D. Dejus, J. Non-Cryst. Solids 106 (1988) p.26.
[21] R. Golovchak, O. Shpotyuk, S. Kozyukhin, A. Kovalskiy, A.C. Miller and H. Jain, J. Appl. Phys. 105 (2009) p.103704.
[22] A. Zeidler, J.W.E. Drewitt, P.S. Salmon, A.C. Barnes, W.A. Crichton, S. Klotz, H.E. Fischer, C.J. Benmore, S. Ramos and A.C. Hannon, J. Phys.: Condens. Matter 21 (2009) p.474217.
[23] R. Holomb, P. Johansson, V. Mitsa and I. Rosola, Philos. Mag. 85 (2005) p.2947.
[24] R. Holomb, N. Mateleshko, V. Mitsa, P. Johansson, A. Matic and M. Veres, J. Non-Cryst. Solids 352 (2006) p.1607.
[25] O. Kondrat, N. Popovich, R. Holomb, V. Mitsa, O. Petrachenkov, M. Koós and M. Veres, Phys. Status Solidi C 7 (2010) p.893.
[26] S.R. Elliot, *Physics of Amorphous Materials*, Longman, New York, NY, 1990.
[27] P. Boolchand, *Insulating and Semiconducting Glasses*, World Scientific, Singapore, 2000.
[28] C. Quémard, F. Smektala, V. Couderc, A. Barthélémy and J. Lucas, J. Phys. Chem. Solids 62 (2001) p.1435.
[29] Q. Liu and X. Zhao, J. Non-Cryst. Solids 256 (2010) p.2375.
[30] V. Mitsa, R. Holomb, M. Veres, A. Marton, I. Rosola, I. Fekeshgazi and M. Koós, Phys. Status Solidi C 8 (1011) p.2696.
[31] R.T. Ananth Kumar, P. Chithra Lekha, B. Sundarakannan and D. Pathinettam Padiyan, Philos. Mag. 92 (1012) p.1422.
[32] K. Shimakawa, A. Kolobov and S.R. Elliott, Adv. Phys. 44 (1995) p.475.
[33] K. Tanaka, J. Non-Cryst. Solids 352 (2006) p.2580.
[34] S. Sugai, Phys. Rev. Lett. 57 (1986) p.456.
[35] V. Petkov and D.Le. Messurier, J. Phys.: Condens. Matter 22 (2010) p.115402.
[36] M. Kibalchenko, J.R. Yates, C. Massobrio and A. Pasquarello, J. Phys. Chem. C 115 (2011) p.7755.
[37] B.N. Ivanov-Emin, J. Gen. Chem. USSR 10 (1940) p.1813.
[38] G. Dittmar and H. Schäfer, Acta Cryst. B 32 (1976) p.1188.
[39] A.V. Novoselova, V.P. Zlomanov, S.G. Karbanov, O.V. Matveyev and A.M. Gas'kov, Prog. Solid State Chem. 7 (1972) p.85.
[40] G. Dittmar and H. Schäfer, Acta Cryst. B 31 (1975) p.2060.
[41] G. Dittmar and H. Schäfer, Acta Cryst. B 32 (1976) p.2726.
[42] G. Lucovsky, R.J. Nemanich and F.L. Galeener, in *Proceedings of the 7th International Conference on Amorphous and Liquid Semiconductors*, W.E. Spear, ed., CICL, Edinburgh, 1977, p.125.
[43] P.M. Bridenbaugh, G.P. Espinosa, J.E. Griffiths, J.C. Phillips and J.P. Remeika, Phys. Rev. B 20 (1979) p.4140.
[44] H. Fjellvåg, K. Ove Kongshaug and S. Stølen, J. Chem. Soc. Dalton Trans. C 61 (2001) p.1043.
[45] J.-E. Kwak and H. Yun, Acta Cryst. C 61 (2005) p.i81.

[46] M. Cobb and D.A. Drabold, Phys. Rev. B 56 (1997) p.3054.
[47] M. Cobb, D.A. Drabold and R.L. Cappelletti, Phys. Rev. B 54 (1996) p.12162.
[48] C. Massobrio, A. Pasquarello and R. Car, Phys. Rev. B 64 (2001) p.144205.
[49] C. Massobrio and A. Pasquarello, Phys. Rev. B 77 (2008) p.144207.
[50] M.J. Frisch, G.W. Trucks, H.B. Schlegel, G.E. Scuseria, M.A. Robb, J.R. Cheeseman, V.G. Zakrzewski, J.A. Montgomery, Jr., R.E. Stratmann, J.C. Burant, S. Dapprich, J.M. Millam, A. D. Daniels, K.N. Kudin, M.C. Strain, O. Farkas, J. Tomasi, V. Barone, M. Cossi, R. Cammi, B. Mennucci, C. Pomelli, C. Adamo, S. Clifford, J. Ochterski, G.A. Petersson, P.Y. Ayala, Q. Cui, K. Morokuma, D.K. Malick, A.D. Rabuck, K. Raghavachari, J.B. Foresman, J. Cioslowski, J.V. Ortiz, A.G. Baboul, B.B. Stefanov, G. Liu, A. Liashenko, P. Piskorz, I. Komaromi, R. Gomperts, R.L. Martin, D.J. Fox, T. Keith, M.A. Al-Laham, C.Y. Peng, A. Nanayakkara, M. Challacombe, P.M.W. Gill, B. Johnson, W. Chen, M.W. Wong, J.L. Andres, C. Gonzalez, M. Head-Gordon, E.S. Replogle, J.A. Pople, Gaussian 03, Revision B.04, Gaussian, Pittsburgh, PA, 2003.
[51] W. Kohn and L.J. Sham, Phys. Rev. 140 (1965) p.A1133.
[52] P.J. Hay and W.R. Wadt, J. Chem. Phys. 82 (1985) p.284.
[53] C.E. Check, T.O. Faust, J.M. Bailey, B.J. Wright, T.M. Gilbert and L.S. Sunderlin, J. Phys. Chem. A 105 (2001) p.8111.
[54] A.D. Becke, Phys. Rev. A 38 (1988) p.3098.
[55] C. Lee, W. Yang and R.G. Parr, Phys. Rev. B 37 (1988) p.785.
[56] H. Appel, E.K.U. Gross and K. Burke, Phys. Rev. Lett. 90 (2003) p.043005.
[57] M.E. Casida, C. Jamorsky, K.C. Casida and D.R. Salahub, J. Chem. Phys. 108 (1998) p.4439.
[58] R.E. Stratmann, G.E. Scuseria and M.J. Frisch, J. Chem. Phys. 109 (1998) p.8218.
[59] C. Massobrio, M. Micoulaut and P.S. Salmon, Solid State Sci. 12 (2010) p.199.
[60] E. Bergignat, G. Hollinger, H. Chermette, P. Pertosa, D. Lohez, M. Lannoo and M. Bensoussan, Phys. Rev. B 37 (1988) p.4506.